CardioMorph Atlas: a statistical approach to evaluate association between pulmonary tuberculosis and cardiac morphology from chest X-rays

Amritpal Singh,[a,b] Sena Azamat,[a] Gourav Modanwal,[c] Pushkar Mutha,[c] Pingfu Fu,[d] Neel R. Gandhi,[e] Rohan Dhamdhere,[c] Mendel Lebowitz,[c] Sadeer Al-Kindi,[g] Anurag Aggarwal,[h] Yingda L. Xie,[f] and Anant Madabhushi[a,b,i,*]

[a]Emory University School of Medicine, Atlanta, USA
[b]Department of Computer Science, Emory University, Atlanta, USA
[c]Department of Biomedical Engineering, Georgia Institute of Technology and Emory University, Atlanta, GA, USA
[d]Department of Population and Quantitative Health Sciences, Case Western Reserve University, USA
[e]Department of Epidemiology, Rollins School of Public Health, Emory University, Atlanta, USA
[f]Department of Medicine and the Public Health Research Institute, Rutgers New Jersey Medical School, USA
[g]Preventive Cardiology, Houston Methodist, USA
[h]Biosciences and Health Research, Ashoka University, India
[i]Atlanta Veterans Administration Medical Center, Atlanta, USA

eBioMedicine
2026;130: 106385
Published Online xxx
https://doi.org/10.1016/j.ebiom.2026.106385

Summary

Background Patients with tuberculosis (TB) face an elevated risk of certain cardiovascular diseases. The inflammatory response associated with TB is linked to cardiac complications, though the spatial impact on cardiac structure remains understudied. In this study, we assess population-level differences in cardiac morphology in TB using an atlas-based approach applied to routine chest X-rays.

Methods A total of 8651 patients (with 2626 patients with TB) were selected from four cohorts: Shenzhen, TBX11K, TB Portals, and MIMIC, covering seven countries. We developed a representative cardiac template, CardioMorph Atlas, and compared population-level morphological differences between patients with TB and controls. Cardiac borders and areas were quantified into CardioMorph features and analysed for their association with all-cause mortality using Cox regression.

Findings CardioMorph Atlas revealed significant lateral elongation of the heart in patients with TB, in both left and right ventricles, with patterns distinct from those in pneumonia and cardiomegaly. Vector field analysis showed lateral extension of cardiac structures in patients with TB. Upper area (hazard ratio: 2.18, 95% CI: 1.1–4.30, p = 0.022) and right perimeter (HR = 2.07, 95% CI:1.06–4.02) were significantly associated with increased all-cause mortality in patients with TB. CardioMorph features showed strong associations with all-cause mortality in patients with TB, supporting their potential utility for risk stratification, and which demonstrates feasibility of quantitatively assessing impact of TB on cardiac morphology using routine chest X-rays.

Interpretation These findings suggest that tuberculosis is linked to distinct, prognostically relevant cardiac morphological alterations detectable on routine chest X-rays using the CardioMorph Atlas. Further prospective validation is warranted.

Funding National Heart, Lung and Blood Institute; National Institute of Allergy and Infectious Diseases.

Keywords: Pulmonary tuberculosis; Cardiac remodelling; Chest X-rays; Imaging biomarkers

Introduction

Tuberculosis (TB) is the leading infectious disease cause of death worldwide,[1] with more than 10 million individuals developing TB disease annually and a million deaths. While the lungs are the most common target in TB, its impact extends beyond the respiratory

*Corresponding author. Emory University, N602, Health Science and Research Building II (HSRB2), Atlanta, GA 30322, USA.
E-mail address: anantm@emory.edu (A. Madabhushi).

Research in context

Evidence before this study

We searched PubMed for studies published in the last five years using the terms "tuberculosis" AND ("heart" OR "cardiac") AND ("X-ray" OR "radiography"). Evidence shows that most research on TB and the heart has focused on direct cardiac involvement, including pericarditis, myocardial infection, or constrictive pericarditis. These studies were primarily case reports, small case series, or specialised imaging studies using MRI, CT, or PET/CT to identify localised cardiac lesions. There is a critical gap in knowledge regarding the effects of pulmonary TB on cardiac morphology and function in the absence of direct cardiac infection, and no large-scale studies have systematically assessed subtle cardiac changes using chest X-rays.

Added value of this study

Using 8651 chest X-rays across four international cohorts, this study demonstrates that pulmonary TB without direct cardiac involvement is associated with measurable cardiac remodelling, including lateral elongation of both ventricles. These changes were captured using a computational morphometric framework, CardioMorph, and were independently associated with all-cause mortality. This represents population-level evidence linking pulmonary TB to subclinical cardiac remodelling and highlights a non-invasive approach to identify individuals at elevated cardiovascular risk.

Implications of all the available evidence

Our findings indicate that pulmonary TB may have systemic cardiovascular consequences even without direct heart infection. Integrating morphometric analysis of routine chest X-rays into TB management could enable early detection of cardiac remodelling and improve risk stratification. These insights expand the understanding of TB as a multisystem disease and could provide a scalable approach for monitoring TB-related cardiac effects in clinical and public health settings.

system, influencing multiple organ systems, including the cardiovascular system.[2] Patients with TB face an elevated risk of cardiovascular disease (CVD) due to both shared risk factors and direct pathophysiological effects of TB on the heart.[3] The chronic inflammatory state induced by TB has been linked to several cardiac complications, yet the precise nature and spatial distribution of TB-related cardiac structural changes remain underexplored.

About 60% of patients with TB show some form of cardiovascular disease, most commonly pericarditis, myocarditis, and coronary artery disease.[4] Pericardial involvement, such as effusion and constrictive pericarditis, is well documented in TB and often causes haemodynamic instability and increased morbidity. TB-related immune responses can also lead to myocardial inflammation and fibrosis, contributing to cardiac dysfunction and heart failure.[4] Cardiac involvement in TB is linked to higher mortality, highlighting the need for early detection and monitoring.[2,5,6] A population study of over 69,000 patients found cardiovascular disease incidence significantly higher (HR = 2.89; 95% CI: 2.58–3.23) in patients with TB treated with standard therapy compared to the general population.[7] Another study[8] showed that patients with pulmonary TB had a 1.5-fold increased risk of aortic complications, like aneurysm and dissection, after adjusting for demographics and comorbidities.

Traditionally, studies investigating TB-related cardiac changes have utilised advanced imaging modalities, such as cardiac magnetic resonance imaging (MRI) and computed tomography (CT) scans.[6,7] These methods provide detailed three-dimensional assessments of cardiac morphology, enabling the identification of ventricular remodelling, myocardial scarring, and pericardial thickening. However, despite their diagnostic accuracy, these imaging techniques are expensive, less accessible, and require specialised expertise,[8] limiting their use in resource-limited settings where TB prevalence is highest.[9,10]

Chest X-rays (CXRs) remain one of the most widely used, cost-effective imaging modalities and are recommended by WHO as a screening and triage tool for evaluating pulmonary TB and other chest-related diseases.[11] Although CXRs are routinely employed for evaluating pulmonary pathology, their application in detecting and quantifying TB-associated cardiac morphological changes has not been extensively explored.

There is increasing interest in understanding whether TB causes structural heart changes, given evidence linking TB to higher cardiovascular risk.[2,5,6] To address this, we developed the **CardioMorph Atlas**, a population-based anatomical framework that captures localised cardiac shape differences related to TB using routine chest X-rays. Built through a multi-step pipeline involving image registration, difference atlas analysis, and vector field modelling, this approach enables systematic comparison of cardiac morphology across cohorts. The first objective of this study was to quantitatively map cardiac deformation patterns associated with TB on chest X-rays. The second was to evaluate the prognostic value of these features, especially their link to all-cause mortality in patients with TB. Together, these aims enhance understanding of TB-related cardiac remodelling and its impact on outcomes. Quantifying heart shape changes with chest X-rays offers population-level insights into TB's cardiovascular effects and provides a scalable imaging-based risk assessment tool. We applied CardioMorph to 8651

CXRs from four large, diverse datasets, including over 2600 patients with TB from Asia, Europe, and North America, covering clinical and population health settings for robust cross-cohort analysis. Although AI has been widely applied to detect pulmonary TB or cardiomegaly on CXRs, our study investigates TB's impact on cardiac anatomy using a population-level, anatomy-based framework. This approach offers a new perspective on systemic disease impact and supports low-cost cardiac monitoring in TB-endemic areas using widely available imaging.

Methods

Cohort creation

In this study, we included retrospectively collected chest X-rays from patients with TB and controls (patients without any reported pulmonary disease) from multiple datasets: the Shenzhen dataset,[12] TBX11K dataset,[13] TB Portals dataset,[14] and the MIMIC dataset,[15] capturing diverse populations across various demographics, including age, sex (self-reported), and ethnic background, which enhances the generalisability of our findings. Acquisition timeframes and data sources for each cohort are summarised in Supplementary Tables S1–S3.

The specific inclusion and exclusion criteria were applied systematically across these cohorts to ensure data quality and diagnostic specificity. For the Shenzhen, TBX11K, and TB Portals datasets, inclusion criteria mandated the availability of 2D chest X-ray images and confirmed disease findings consistent with either active tuberculosis or absence of any reported pulmonary disease. Conversely, for the MIMIC dataset, inclusion required 2D chest X-ray images exhibiting findings of Pneumothorax, Cardiomegaly, or Atelectasis. Across all four cohorts, cases identified as latent tuberculosis were excluded. Since valid segmentation is a prerequisite for all downstream morphometric measurements, scans where the pre-trained segmentation model failed to localise the heart or lungs were additionally excluded (less than 1% of all scans). Fig. 1 details patient selection. The Shenzhen, TBX11K, and TB Portals datasets consist predominantly of posteroanterior (PA) erect acquisitions; the MIMIC dataset contains a mixture of PA and anteroposterior (AP) projections. The CardioMorph Atlas was created using data from Cohorts 1 (Shenzhen) and 2 (TBX11K), including patients with active TB and controls to capture cardiac morphological variations linked to pulmonary disease. In this work, patients without any reported pulmonary finding were referred to as controls. Cohort 1 had 658 patients (335 with active TB, 323 controls), while Cohort 2 included 4767 patients (969 active TB, 3798 controls) selected from a larger pool. Cohort 3 (TB Portals) had 1322 patients with active TB for analysing the prognostic role of cardiac involvement via all-cause mortality. Cohort 4 (MIMIC) comprised 1904 patients with non-TB thoracic conditions 500 with cardiomegaly, 500 pneumonia, 328 pneumothorax, 76 atelectasis and 500 controls, used to build a non-TB atlas for differential diagnosis. The phenotype label harmonised terminology and atlas names is detailed in Supplementary Fig. S1 and Table S4.

CardioMorph Atlas creation

CardioMorph quantifies population-level cardiac shape variation directly from chest X-ray silhouettes, defining morphological phenotypes independently of clinical cardiac disease classification. CardioMorph Atlas creation involved four steps: region of interest segmentation, template selection, image registration, and atlas generation. Lung and heart chambers were segmented using a pre-trained model,[16] images cropped to the thoracic cavity, and resized to 512 × 512 pixels to standardise field of view. A representative cardiac template was chosen based on the median heart area from the control cohort to ensure that the baseline measurements were taken from the control group. This template serves as a reference for comparing the structural differences in patients with TB. All X-rays were first registered using a rigid registration and followed by affine registration to a canonical frame with DICE scores assessing alignment accuracy, explicitly correcting for translation, rotation, and scaling differences arising from variation in patient posture and projection geometry. As the atlas is derived from population-level averaging of signed distance maps, random inter-individual positional variation is expected to cancel out, with only consistent, systematic shape differences surviving permutation-corrected group-level statistical comparison.

Binary heart chamber masks were converted to signed distance functions, and TB vs. control differences were quantified via GLM-based t-tests with permutation testing and multiple-comparison correction. Representative signed distance function templates for the TB and control groups are shown in Supplementary Figs. S2, S5–S7.

Displacement vector field analysis

To understand the direction and extent of changes in cardiac structure associated with tuberculosis, we quantified TB-associated cardiac shape changes using pixel-wise displacement vector field analysis on chest X-rays. Heart contours of TB and control groups were aligned via B-spline transformation,[17] and resulting vectors (direction and magnitude) were averaged within a polar grid of concentric zones and angular sectors to map regional deformations.

Feature generation

CardioMorph features were derived from four landmark points per heart chamber, enabling border and

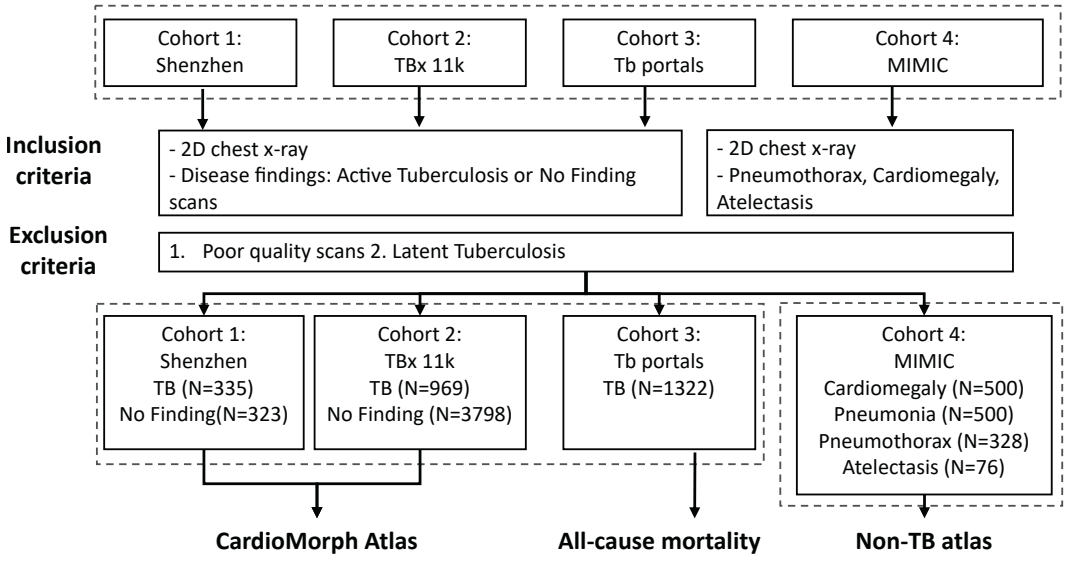

Fig. 1: **Cohort diagram with inclusion and exclusion criteria for the atlas creation and all-cause mortality analysis.**

area measurements as 2D/3D morphology proxies. These features capture geometric and spatial cardiac variations and were compared across TB vs. controls using the Wilcoxon rank-sum test. Fig. 2 illustrates the different cardiac chambers and the methodology used to extract the cardiac borders and areas features.

All-cause mortality

Overall survival was measured from TB diagnosis to death, with patients split into Cardiac-high and Cardiac-low groups by median CardioMorph feature values. A 6-month landmark Kaplan–Meier and Cox regression analysis assessed the prognostic impact of cardiac morphology changes, reporting hazard ratios, confidence intervals, and p-values. Prognostic analyses were performed on the full TB Portals cohort (n = 1322 patients with active TB); survival metadata, including comorbidities, were available for n = 688, in whom multivariable Cox models were fitted. Baseline demographic and clinical characteristics are presented in Supplementary Table S5.

Statistics

All statistical analyses were performed using Python 3.8. Cardiac morphological differences between patients with active TB and controls were assessed using the Wilcoxon rank-sum test, a non-parametric test chosen given the non-normal distribution of morphometric measurements across cohorts. The CardioMorph Atlas was constructed using generalised linear model (GLM)-based t-tests[18] with permutation testing (n = 500 permutations) and multiple-comparison correction to identify regions of statistically significant shape difference; this approach is established for population-level image-based morphometry and was selected for its robustness to non-Gaussian spatial data. All-cause mortality analyses were performed using Kaplan–Meier estimation and Cox proportional hazards regression. A 6-month landmark was applied to reduce immortal time bias. Univariate Cox models were fitted for individual CardioMorph features; multivariable models additionally adjusted for age, sex, BMI, country of origin, HIV status, drug resistance, Hepatitis C status, diabetes, TB site, and lung localisation. Hazard ratios with 95% confidence intervals and two-sided p-values are reported throughout; $p < 0.05$ was considered statistically significant.

Ethics

This study used only retrospective secondary analysis of fully de-identified, publicly available chest X-rays datasets (Shenzhen, TBX11K, TB Portals, and MIMIC-CXR), with no direct patient contact or new data collection. All studies involved exclusively de-identified public data. All original datasets were collected with appropriate ethical approvals and informed consent as described in their respective primary publications. Access to TB Portals and MIMIC-CXR was obtained through approved data use agreements, and the requirement for additional informed consent was waived due to the use of de-identified data.

Role of funders

The funders of the study had no role in experimental design, data collection, data analysis, data interpretation, or writing of the study.

Results

A total of 8651 patients were included from multiple retrospective cohorts, encompassing a diverse population

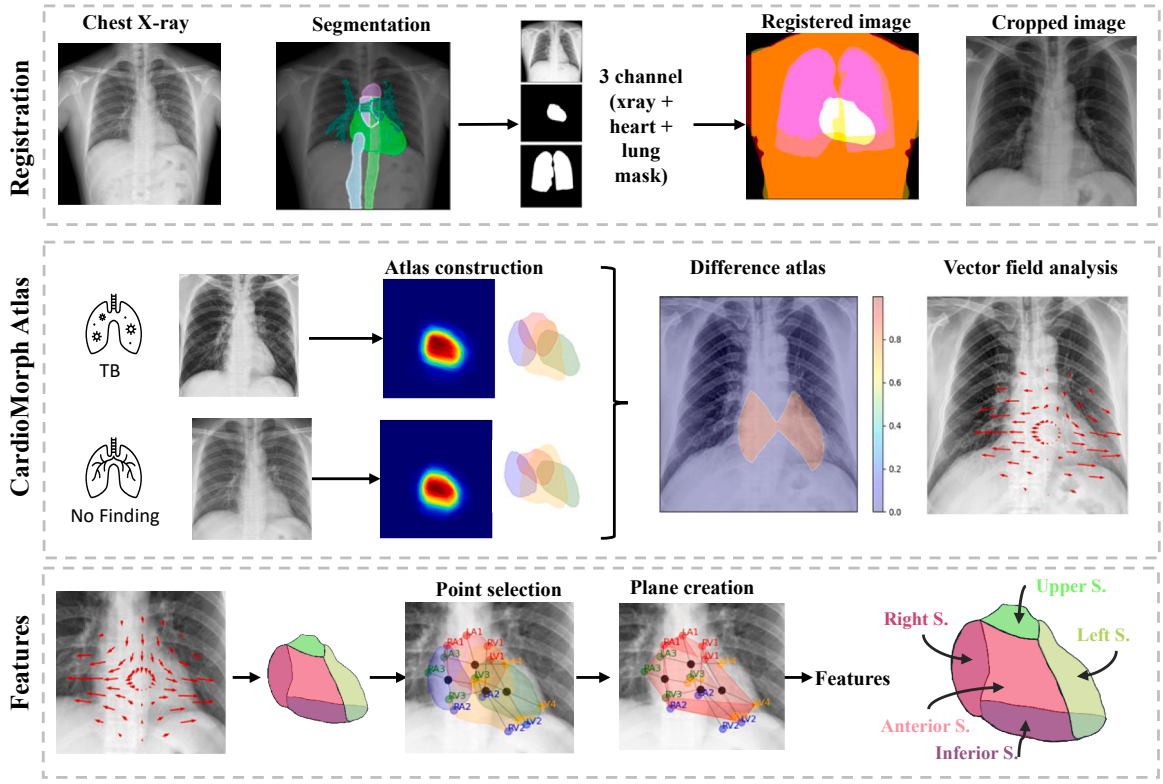

Fig. 2: **Workflow diagram with steps to summarise population-level differences into the CardioMorph Atlas.**

across seven countries and multiple ethnicities, as shown in Fig. 3. The cohort distribution was as follows: 4767 patients from the TBX11K dataset[13] (TB/controls 969/3798), 658 patients from the Shenzhen dataset[12] (TB/controls: 335/323), 1322 patients from the TB Portals dataset,[14] all of whom were TB-positive (TB/controls: 1322/0), and 1904 patients from the MIMIC dataset,[15] representing a range of clinical conditions. Inclusion and exclusion criteria are detailed in Fig. 1. A detailed breakdown of patient numbers by disease category and dataset is provided in Fig. 4 and Supplementary Table S2.

Evaluating cardiac differences in patients with TB

To ensure accurate anatomical alignment of cardiac structures across all X-rays images, a robust image registration pipeline was implemented. The registration accuracy, measured using the DICE score, achieved a value of 0.841 for heart-to-heart alignment. This high level of accuracy confirmed that the cardiac morphology across all images was consistently aligned, allowing meaningful shape-based comparisons.

To compare shape variation between patients with TB and controls, we created the difference atlas (D_{TB}).

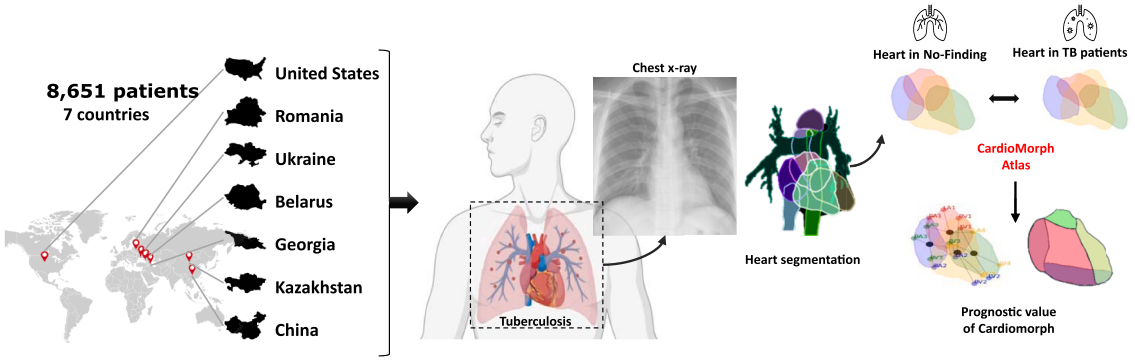

Fig. 3: **Main overview illustrates the creation of the CardioMorph Atlas, including segmentation of cardiac substructures to detect morphological changes in tuberculosis patients.**

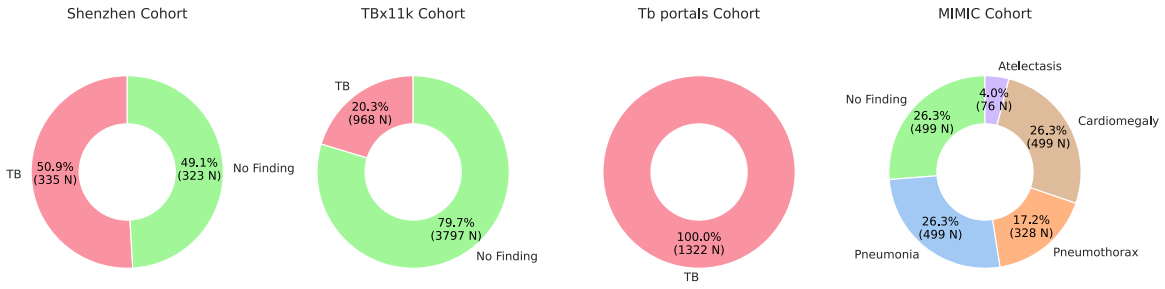

Fig. 4: **Patient scan count and disease distribution across different datasets used in this study.**

This generates a heatmap of areas with significant morphological differences. Across both Shenzhen and TBX11K datasets, multiple regions of the heart exhibited significant morphological differences, predominantly located along the lateral borders of the heart, as observed in Fig. 5.

To further examine the structural alterations observed in patients with TB, vector field analysis was performed as detailed in Fig. 5. The displacement vectors from controls to patients with TB showed a lateral outward expansion of the heart, suggesting that TB is associated with an overall widening of the cardiac silhouette. This finding was consistent across all datasets and closely aligned with the differences detected in the difference atlas. The magnitude of the vectors corresponded to the extent of morphological differences, while the direction of the vectors indicated the precise nature of the shape deformation.

On quantification of cardiac structures further into CardioMorph features, several features demonstrated statistically significant differences between patients with TB and controls across the Shenzhen and TBX11K datasets on univariate analysis. On multivariable analysis adjusting for age, sex, BMI, country, HIV status, drug resistance, Hepatitis C, diabetes, TB site, and lung localisation, CardioMorph features remained independently associated with all-cause mortality, indicating that the prognostic signal is not explained by disease severity or comorbidity burden (Supplementary Table S7). The left border length and left cardiac area were consistently larger in TB compared to controls ($p < 0.001$ for both metrics in both datasets). These results suggest that TB is associated with an enlargement of the left side of the heart, which may be driven by ventricular hypertrophy or increased workload on the left ventricle. The descriptive statistics for these

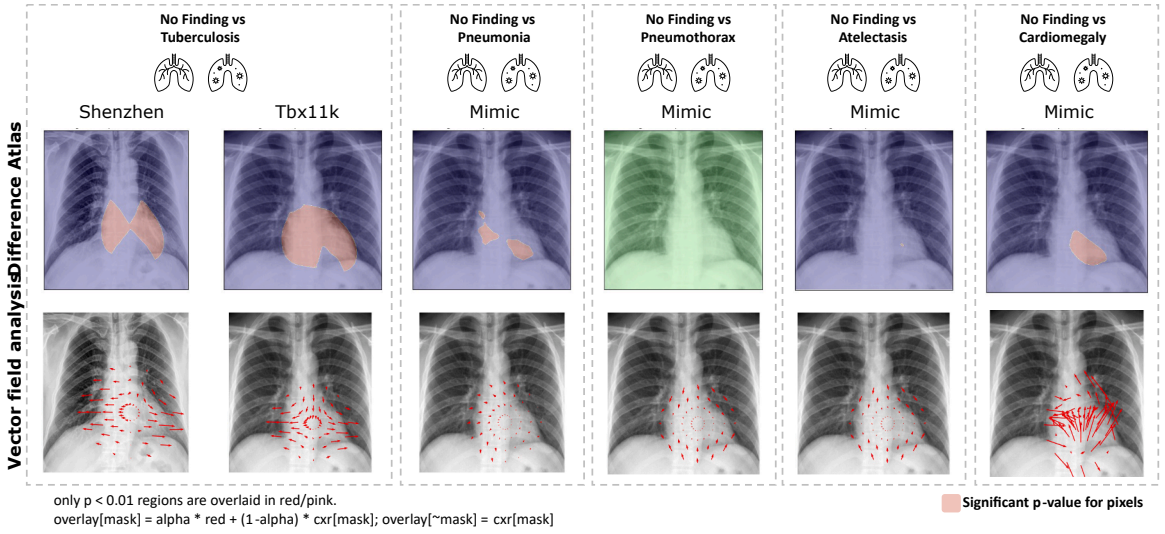

Fig. 5: **Difference atlas for tuberculosis and other diseases.** Red/pink overlay regions denote pixels where the signed-distance-function difference between groups reached statistical significance ($p < 0.01$, GLM-based t-test with permutation testing and FDR correction). Non-significant regions display the underlying chest X-ray without colour overlay. The bottom row shows vector-field analysis overlaid on the same panels, with arrow direction and length indicating the direction and magnitude of local cardiac shape displacement between groups.

morphological features across different cohorts are summarised in Table 1.

Comparing cardiac differences with Non-TB conditions

To assess whether these cardiac shape differences were unique to tuberculosis, we generated difference atlases for pneumonia, atelectasis, and pneumothorax patients from the MIMIC dataset. These groups showed no similar structural alterations, suggesting TB-specific deformations. For comparison with cardiomegaly, a separate atlas (D_{Cmeg}) revealed localised left ventricular changes, unlike the diffuse, lateral enlargement in TB, consistent with known cardiomegaly patterns[19,20](Fig. 5). Pneumonia, atelectasis, and pneumothorax patients had only small, randomly oriented displacement vectors, while cardiomegaly vectors pointed toward the left ventricular apex, matching classic enlargement patterns. This is in marked contrast to the TB-associated pattern, which showed consistent, bilaterally directed lateral displacement vectors of substantially greater magnitude, indicative of a diffuse, symmetric cardiac remodelling process rather than positional displacement.[21] Notably, conditions such as pneumothorax and atelectasis which are known to cause mediastinal shift and could therefore be expected to produce directional cardiac displacement,[22] instead yielded non-directional, low-magnitude vectors in this cohort, further supporting the specificity of the TB-associated deformation pattern. These contrasts underscore the distinct remodelling pattern of TB compared to other pulmonary and cardiac conditions.[19] Supplementary Figs. S5 and S6 provide a detailed visualisation of the vector field analysis across different heart chambers and disease categories.

Prognostic analysis of CardioMorph features in patients with TB

We stratified TB Portals patients into CardioMorph-positive (CM+) and CardioMorph-negative (CM–) groups based on whether cardiac morphological features exceeded the population median. CM + patients had significantly higher mortality than CM– (Fig. 6). On univariate landmark analysis, increased upper area predicted higher all-cause mortality (HR = 2.18, 95% CI: 1.1–4.30, p = 0.022), as did increased upper perimeter (HR = 2.07, 95% CI: 1.06–4.02, p = 0.029), possibly reflecting aortic root dilation or cardiac strain.[10] Conversely, decreased right perimeter was linked to lower mortality risk (HR = 0.42, 95% CI: 0.21–0.84, p = 0.011), suggesting reduced remodelling or pulmonary hypertension. As mentioned previously, these findings were significant despite adjusting for age, sex, BMI, country, HIV status, drug resistance, Hepatitis C, diabetes, TB site, and lung localisation (More details on different adjusted models can be found in Supplementary Tables S6–S8, and Supplementary Figs. S3 and S4).

Feature class	Cohort 1 (Shenzhen)	Cohort 2 (TBX11K)
Areas		
Upper	0.249	**<0.001**
Anterior	**<0.001**	**<0.001**
Inferior	0.841	**<0.001**
Left	**<0.001**	**<0.001**
Right	**<0.001**	**<0.001**
Perimeter		
Upper	0.37	0.352
Anterior	**<0.001**	**<0.001**
Inferior	**<0.001**	**<0.001**
Left	**<0.001**	**<0.001**
Right	**0.019**	**<0.001**

Student's t-test p-values reported. Significant values are bold.

Table 1: **Comparison of CardioMorph features in patients with TB and 'no finding' controls across Shenzhen and TBX11K datasets.**

Discussion

Pulmonary tuberculosis increases CVD risk,[3,23,24] but its spatial and structural cardiac effects remain poorly quantified with accessible imaging. This study tested whether computational analysis of routine CXRs could detect consistent changes and inform prognosis. Using four datasets, we developed a population-based modelling framework to register images, created a CardioMorph Atlas, and mapped structural differences between patients with TB and controls. Vector field analysis quantified deformation direction and magnitude, and CardioMorph features were extracted for statistical and prognostic evaluation.

Population-based morphometric analysis enables localised assessments of structural variation by aligning anatomies to a reference and analysing deviations.[25,26] Though common in MRI and neuroimaging, it has been applied in brain,[26–28] lung,[29,30] and prostate[31] studies and lung region detection.[32,33] This framework allows the measurement of TB-related cardiac changes using 2D CXRs. Our tailored registration pipeline produced the CardioMorph Atlas, integrating vector field analysis with morphology metrics, demonstrating a low-cost, scalable method for studying systemic disease effects on cardiac structure.

CardioMorph difference maps and vector field analysis reveals significant lateral elongation of the heart in patients with TB, as illustrated in Fig. 5. CardioMorph analysis showed significant lateral elongation in patients with TB, affecting both ventricles rather than just the left ventricle as in cardiomegaly, suggesting diffuse structural impact. Univariate analysis revealed increased left heart border length and upper area, potentially indicating aortic root dilation, consistent with evidence linking TB to higher risk of aortic complications. Chronic inflammation, pulmonary hypertension, and vascular remodelling may drive the

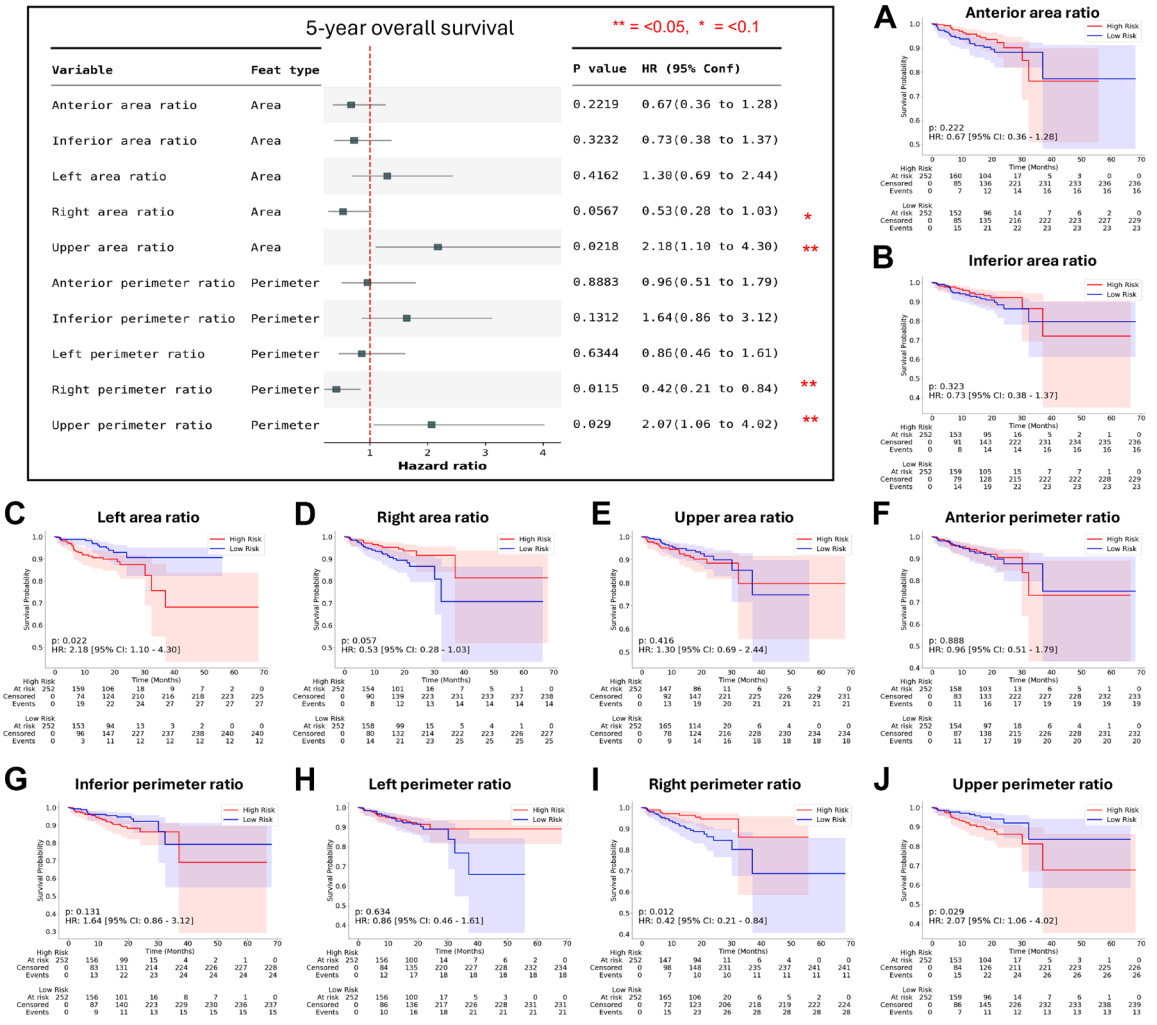

Fig. 6: **(A) Forest plots and KM curves (A–J) for all-cause mortality using cardiac features on the TB Portals dataset**.

ventricular hypertrophy and deformation, with effects on extracellular matrix, fibrosis, and compliance. These findings point to multifactorial remodelling in TB, highlight cardiac morphology as a potential prognostic marker, and underscore the need for longitudinal studies to assess progression and functional impact.

TB-induced cardiac alterations appear distinct from those in other diseases like pneumonia and cardiomegaly, suggesting a unique impact of TB on the cardiovascular system. Understanding these differences can improve diagnostic accuracy, helping clinicians distinguish TB-related heart changes from other cardiac conditions. Identifying specific morphological markers for TB could enable earlier detection of cardiovascular involvement, allowing for timely interventions and better outcomes. Supplementary Fig. S8 shows our hypothesised pathophysiological pathway linking TB to cardiac changes.

Enlargement of both ventricles, especially the left, is a key finding in patients with TB. While left ventricular enlargement can resemble cardiomegaly, the mechanisms in TB may differ. Increased workload on the left ventricle, likely due to elevated cardiac resistance,[34,35] could be a probable cause. Pulmonary TB complications such as fibrosis and cavitation can lead to pulmonary hypertension, increasing cardiac strain. This strain typically peaks around six months post-infection as inflammation sustains pressure on the heart, resulting in ventricular enlargement[36,37] and left ventricular hypertrophy from increased vascular resistance.[34,35] Whilst TB-related fibrosis and collapse can cause ipsilateral mediastinal shift,[22] the observed bilateral symmetric cardiac elongation is mechanistically inconsistent with unilateral displacement, supporting intrinsic cardiac remodelling as the predominant driver.

Finally, while this study provides a valuable starting point for understanding the cardiac impact of TB, it is important to note that there are still many unanswered questions. In this work, we find that the changes in upper area, upper perimeter, and right perimeter of the entire heart were associated with increased all-cause mortality in patients with TB. A 2020 meta-analysis reported 51% higher risk of major adverse cardiac events in TB survivors, emphasising the prognostic importance of detecting early remodelling.[23] The exact mechanisms behind the observed lateral elongation of the heart and other morphological changes remain unclear. Further research is needed to fully elucidate the biological processes driving these alterations and to determine how they relate to clinical outcomes in patients with TB. As our understanding of the relationship between TB and cardiac morphology improves, we may be able to develop more effective strategies for preventing and managing TB-related cardiovascular disease, improving the prognosis for affected individuals.

This study highlights cardiac morphological changes in patients with TB but has limitations that affect robustness and generalisability. Heterogeneity in acquisition protocol across cohorts including projection type (PA vs. AP) and patient positioning represents a residual limitation not fully resolved by registration. Retrospective datasets may introduce selection bias, and the absence of serial imaging limits understanding of temporal progression. Lack of cause-specific mortality data hinders assessment of TB-related deaths, and batch effects between TB and non-TB datasets could inflate model performance. In the absence of uniform severity scores across public datasets, TB site and lung localisation were employed as structured proxies for disease extent; future prospective studies should incorporate standardised radiographic severity scoring. Diabetes prevalence in the TB Portals cohort was relatively low (5.1%), limiting power to exclude residual confounding from diabetic cardiomyopathy[38] a well-characterised cause of left ventricular hypertrophy.

Furthermore, conditions included in the MIMIC comparison group specifically pneumothorax and atelectasis are known to cause mediastinal shift, which may alter cardiac position and apparent size on chest X-rays; whilst the observed displacement vectors in these groups were small and non-directional, future studies should prospectively exclude cases with radiographically confirmed significant mediastinal displacement to further strengthen specificity analyses. Fibrosis or collapse-driven mediastinal shift in advanced TB may contribute residual cardiac displacement not fully resolved by registration; future studies should stratify by radiographic extent of parenchymal disease.

Causality could not be determined, only correlations. Future work should use prospective cohorts with longitudinal imaging, assess specific mortality causes, and validate findings with advanced modalities (CT/MRI) to capture 3D changes. TB-related cardiac strain may vary with infection severity, comorbidities, immune status, and disease duration; examining these factors could improve risk stratification and guide targeted interventions for high-risk patients.

This study demonstrates the potential of chest X-rays as a non-invasive, cost-effective tool to detect cardiac morphological changes in patients with TB. Using difference atlas and vector field analysis, we identified TB-specific cardiac deformation patterns distinct from conditions like cardiomegaly and pneumonia. Changes in the upper and right heart perimeter were linked to all-cause mortality, highlighting their prognostic value.

These results suggest that cardiac morphology features could improve early detection and risk stratification of TB-related cardiac involvement, potentially enhancing patient outcomes. However, further validation through prospective, longitudinal studies is needed, along with investigation into the mechanisms driving these changes. In summary, this work shows the feasibility of using chest X-rays and advanced computational methods to assess cardiac morphology in patients with TB. Future efforts should focus on clinical validation and integration into practice to better manage TB and reduce cardiovascular complications.

Contributors

AS, SA, PM, PF, NG, GM, RD, ML, YX, SA-K, AA, and AM contributed to the conception and design of the study. AS led data curation, performed statistical analysis, interpreted the results, and drafted the manuscript. PM and GM contributed to the development and implementation of the computational pipelines. PF provided biostatistical expertise and contributed to the statistical methodology. NG, YX, SA-K, and AA contributed to clinical interpretation of the findings. SA, PM, PF, NG, GM, RD, ML, YX, SA-K, and AA contributed to data analysis, interpretation, and critical revision of the manuscript. AM provided overall scientific direction, supervised study design and analyses, and critically revised the manuscript. AS and AM accessed and verified the underlying data. All authors contributed to manuscript writing, provided critical intellectual input, had access to the study data, and approved the final version of the manuscript.

AS: Amritpal Singh; SA: Sena Azamat; PM: Pushkar Mutha; PF: Pingfu Fu; NG: Neel R Gandhi; GM: Gourav Modanwal; RD: Rohan Dhamdhere; ML: Mendel Lebowitz; YX: Yingda Xie; SA-K: Sadeer Al Kindi; AA: Anurag Aggarwal; AM: Anant Madabhushi.

Data sharing statement

This study used exclusively publicly available, de-identified datasets. No new primary data were collected. The chest X-rays datasets used are available as follows: the Shenzhen dataset is freely accessible via the National Library of Medicine (https://lhncbc.nlm.nih.gov/LHC-research/LHC-projects/image-processing/tuberculosis-chest-x-ray-image-data-sets.html). The TBX11K dataset is available at https://mmcheng.net/tb/. The TB Portals dataset is accessible following registration and approval of a data access request at https://tbportals.niaid.nih.gov/access-data. The MIMIC-CXR dataset requires completion of a credentialing process and a signed data use agreement via PhysioNet at https://physionet.org/content/mimic-cxr/view-dua/2.1.0/. Code is available at https://github.com/Amritpal-001/cardiomorph.

Requests for further information on data access or analysis should be directed to the corresponding author, Anant Madabhushi, PhD, at anantm@emory.edu.

Declaration of interests

AM is a Research Career Scientist at the Atlanta Veterans Affairs Medical Centre, an equity holder in Picture Health, Elucid Bioimaging, and Inspirata Inc. Currently, he serves on the advisory board of Picture Health. He currently consults for Takeda Inc. He also has sponsored research agreements with AstraZeneca and Bristol Myers-Squibb. His technology has been licenced to Picture Health and Elucid Bioimaging. All other authors have no interests to declare.

Acknowledgements

Research reported in this publication was supported by the National Cancer Institute under award numbers - R01CA249992 - 01A1, R01CA257612 - 01A1, R01CA264017 - 01, R01CA268287 - 01A1, U01CA113913 - 16A1, U01CA269181 - 01, U24CA274494-01; U54CA302465-01; R01CA268207-01; the National Heart, Lung, and Blood Institute under award numbers - R01HL158071 - 01A1; the National Institute of Allergy and Infectious Diseases under award number - R01AI175555 - 01A1 and R01HL151277 - 01A1, the National Institute of Biomedical Imaging and Bioengineering under award number 75N92022D00015; the National Library of Medicine under award number - R01LM013864 - 01A1; the National Institute on Aging under award number - R01AG089759; the National Institute of Diabetes and Digestive and Kidney Diseases under award number - R01DK118431; the Office of the Director, National Institutes of Health under award number 1OT2OD038065-01; the Kidney Mapping and Atlas Project (KMAP) under award number - U01DK133090 - 01; the United States Department of Veterans Affairs VA Merit Review award under award number - IBX004121; the VA Biomedical Laboratory Research and Development Service under award numbers - I01CX002622, I01CX002776, IK6BX006185. The VA Research and Development Office through the Lung Precision Oncology Program - LPOP-L0021; the Kidney Mapping and Atlas Project (KMAP) under award number - U01DK133090-01; the Advanced Research Projects Agency for Health (ARPA-H) under award number D25CA00140-00; and sponsored research agreements from AstraZeneca, Bristol Myers Squibb, the Prevent Cancer Foundation, Innovation in Cancer Informatics, the Institute for Technology in Health Care, the Breast Cancer Research Foundation and the Scott Mackenzie Foundation. The content is solely the responsibility of the authors and does not necessarily represent the official views of the National Institutes of Health, the U.S. Department of Veterans Affairs, or the United States Government. During the preparation of this work the authors used Claude (Anthropic) in order to refine language and improve readability. The authors have reviewed and confirmed the validity of the text and take full responsibility for the content of the publication.

Appendix A. Supplementary data

Supplementary data related to this article can be found at https://doi.org/10.1016/j.ebiom.2026.106385.

References

1 *Global tuberculosis report*; 2025. https://www.who.int/publications/i/item/9789240116924.
2 López-López JP, Posada-Martínez EL, Saldarriaga C, et al. Tuberculosis and the heart. *J Am Heart Assoc*. 2021;10:e019435.
3 Huaman MA, Henson D, Ticona E, Sterling TR, Garvy BA. Tuberculosis and cardiovascular disease: linking the epidemics. *Trop Dis Travel Med Vacc*. 2015;1:10.
4 Marcu DTM, Adam CA, Mitu F, et al. Cardiovascular involvement in tuberculosis: from pathophysiology to diagnosis and complications—A narrative review. *Diagnostics (Basel)*. 2023;13:432.
5 Dasgupta S, Kelleman M, Slesnick T, Oster ME. Cardiomegaly on chest radiographs as a predictor of heart disease in the pediatric population. *Am J Emerg Med*. 2020;38:855–859.
6 Aderinto N. Diagnosing the disparities: an analysis of the current state of medical imaging in Africa and strategies for improvement: a correspondence. *International Journal of Surgery: Global Health*. 2023;6:e138.
7 Oh DK, Jo KW, Kim YJ, et al. Risk of cardiovascular event and influence of pyrazinamide in patients with active TB in South Korea: a population-based cohort study. *CHEST*. 2017;152:A199.
8 Chen M-T, Chung CH, Ke HY, Peng CK, Chien WC, Shen CH. Risk of aortic aneurysm and dissection in patients with tuberculosis: a nationwide population-based cohort study. *Int J Environ Res Public Health*. 2021;18:11075.
9 Ardekani S, Weiss RG, Lardo AC, et al. Computational method for identifying and quantifying shape features of human left ventricular remodeling. *Ann Biomed Eng*. 2009;37:1043–1054.
10 Backhaus SJ, Nasopoulou A, Lange T, et al. Left atrial roof enlargement is a distinct feature of heart failure with preserved ejection fraction. *Circ Cardiovasc Imaging*. 2024;17:e016424.
11 Lakshmanan S, Mbanze I. A comparison of cardiovascular imaging practices in Africa, North America, and Europe: two faces of the same coin. *European Heart Journal - Imaging Methods and Practice*. 2023;1:qyad005.
12 Jaeger S, Candemir S, Antani S, Wáng YX, Lu PX, Thoma G. Two public chest X-ray datasets for computer-aided screening of pulmonary diseases. *Quant Imaging Med Surg*. 2014;4:475–477.
13 Liu Y, Wu YH, Zhang SC, Liu L, Wu M, Cheng MM. Revisiting computer-aided tuberculosis diagnosis. *IEEE Trans Pattern Anal Mach Intell*. 2024;46:2316–2332.
14 Rosenthal A, Gabrielian A, Engle E, et al. The TB portals: an open-access, web-based platform for global drug-resistant-tuberculosis data sharing and analysis. *J Clin Microbiol*. 2017;55:3267–3282.
15 Johnson AEW, Pollard TJ, Berkowitz SJ, et al. MIMIC-CXR, a de-identified publicly available database of chest radiographs with free-text reports. *Sci Data*. 2019;6:317.
16 Seibold C, Jaus A, Fink MA, et al. Accurate fine-grained segmentation of human anatomy in radiographs via volumetric pseudo-labeling. *arXiv*. 2023. https://doi.org/10.48550/arXiv.2306.03934.
17 Bae SH, Go S, Kim J, Park KH, Lee S, Park SJ. A novel vector field analysis for quantitative structure changes after macular epiretinal membrane surgery. *Sci Rep*. 2024;14:8242.
18 Nichols TE, Holmes AP. Nonparametric permutation tests for functional neuroimaging: a primer with examples. *Hum Brain Mapp*. 2002;15:1–25.
19 Amin H, Siddiqui WJ. Cardiomegaly. In: *StatPearls*. Treasure Island (FL): StatPearls Publishing; 2025.
20 Elrod JW, van Berlo JH. Unraveling the complexities of cardiac remodeling and hypertrophy — high-content screening and computational modeling. *J Mol Cell Cardiol*. 2014;72:360–363.
21 Byrne A, Al-Hindawi Y, Plit M, et al. The prevalence and pattern of post tuberculosis lung disease including pulmonary hypertension from an Australian TB service; a single-centre, retrospective cohort study. *BMC Pulm Med*. 2025;25:84.
22 Rehaman A, Ramesh A, Prajapati S, Basavappa R. Lead displacement due to tension pneumothorax following permanent pacemaker implantation. *J Cardiol Cases*. 2017;15:25–27.
23 Basham CA, Smith SJ, Romanowski K, Johnston JC. Cardiovascular morbidity and mortality among persons diagnosed with tuberculosis: a systematic review and meta-analysis. *PLoS One*. 2020;15:e0235821.
24 Patil SV, Toshniwal S, Acharya A, Gondhali G. Cardiac dysfunction in active pulmonary tuberculosis: mysterious facts of TB's pandora. *Electron J Gen Med*. 2023;20:em452.
25 Manjón JV, Morell-Ortega S, Ruiz-Perez M, et al. Ultra-high resolution multimodal MRI densely labelled holistic structural brain atlas. *arXiv*. 2025. https://doi.org/10.48550/arXiv.2501.16879.
26 BachCuadra M, Pollo C, Bardera A, Cuisenaire O, Villemure JG, Thiran JP. Atlas-based segmentation of pathological MR brain images using a model of lesion growth. *IEEE Trans Med Imaging*. 2004;23:1301–1314.
27 Cao Y. Atlas based segmentation by diffeomorphic deformation. In: *2008 international conference on wavelet analysis and pattern recognition*. vol. 1. 2008:118–122.
28 Cuadra MB, Pollo C, Bardera A, Cuisenaire O, Villemure JG, Thiran JP. Atlas-based segmentation of pathological MR brain images using a model of lesion growth. *IEEE Trans Med Imag*. 2004;23(10):1301–1314. https://doi.org/10.1109/TMI.2004.834618.
29 Hiremath A, Yuan L, Shiradkar R, et al. LuMiRa: an integrated lung deformation atlas and 3D-CNN model of infiltrates for COVID-19 prognosis. In: *Medical Image Computing and Computer Assisted Intervention – MICCAI 2021: 24th International Conference, Strasbourg, France, September 27 – October 1, 2021, Proceedings, Part VII*. Springer-Verlag; 2021:367–377. https://doi.org/10.1007/978-3-030-87234-2_35.
30 Munoz E, Baudot P, Le VK, et al. 3D-Morphomics, Morphological Features on CT scans for lung nodule malignancy diagnosis. In: Ali S, et al. eds. *Cancer Prevention Through Early Detection*. Cham: Springer Nature Switzerland; 2022:3–13. https://doi.org/10.1007/978-3-031-17979-2_1.
31 Shiradkar R, Ghose S, Mahran A, et al. Prostate surface distension and tumor texture descriptors from pre-treatment MRI are

associated with biochemical recurrence following radical prostatectomy: preliminary findings. *Front Oncol*. 2022;12:841801.
32 Tustison NJ, Qing K, Wang C, Altes TA, Mugler JP III. Atlas-based estimation of lung and lobar anatomy in proton MRI. *Magn Reson Med*. 2016;76:315–320.
33 Zhang L, Hoffman EA, Reinhardt JM. Atlas-driven lung lobe segmentation in volumetric X-ray CT images. *IEEE Trans Med Imaging*. 2006;25:1–16.
34 Han Y, Li Y, Wu Z, et al. Progress in diagnosis and treatment of hypertension combined with left ventricular hypertrophy. *Ann Med*. 2024;56:2405080.
35 Kunišek J, Kunišek L. Impact of blood pressure components on left ventricular hypertrophy remodeling. *Acta Clin Croat*. 2018;57:638–645.
36 Hnizdo E, Singh T, Churchyard G. Chronic pulmonary function impairment caused by initial and recurrent pulmonary tuberculosis following treatment. *Thorax*. 2000;55:32–38.
37 Kim LB, Putyatina AN. Mechanism of lungs fibrosis in mycobacterial infection. *Explor Med*. 2023;4:956–976.
38 Mohan M, Dihoum A, Mordi IR, Choy AM, Rena G, Lang CC. Left ventricular hypertrophy in diabetic cardiomyopathy: a target for intervention. *Front Cardiovasc Med*. 2021;8:746382.